Biochemical and Biophysical Research Communications 438 (2013) 697–702

Contents lists available at ScienceDirect

Biochemical and Biophysical Research Communications

journal homepage: www.elsevier.com/locate/ybbrc

Honokiol inhibits pathological retinal neovascularization in oxygen-induced retinopathy mouse model

Divya Teja Vavilala [a,1], Bliss E. O'Bryhim [b,1], V.K. Chaithanya Ponnaluri [a], R. Sid White [b], Jeff Radel [b], R.C. Andrew Symons [b,c,d], Mridul Mukherji [a,*]

[a] Division of Pharmaceutical Sciences, School of Pharmacy, University of Missouri-Kansas City, MO, USA
[b] Department of Ophthalmology, University of Kansas Medical Center, Kansas City, KS, USA
[c] Ophthalmology Department, Royal Melbourne Hospital, University of Melbourne, Victoria, Australia
[d] Department of Surgery, Royal Melbourne Hospital, University of Melbourne, Victoria, Australia

ARTICLE INFO

Article history:
Received 27 July 2013
Available online 3 August 2013

Keywords:
Hypoxia signaling
Transcription regulation
OIR-model
Angiogenesis
Honokiol
Retinopathy

ABSTRACT

Aberrant activation of the hypoxia inducible factor (HIF) pathway is the underlying cause of retinal neovascularization, one of the most common causes of blindness worldwide. The HIF pathway also plays critical roles during tumor angiogenesis and cancer stem cell transformation. We have recently shown that honokiol is a potent inhibitor of the HIF pathway in a number of cancer and retinal pigment epithelial cell lines. Here we evaluate the safety and efficacy of honokiol, digoxin, and doxorubicin, three recently identified HIF inhibitors from natural sources. Our studies show that honokiol has a better safety to efficacy profile as a HIF inhibitor than digoxin and doxorubicin. Further, we show for the first time that daily intraperitoneal injection of honokiol starting at postnatal day (P) 12 in an oxygen-induced retinopathy (OIR) mouse model significantly reduced retinal neovascularization at P17. Administration of honokiol also prevents the oxygen-induced central retinal vaso-obliteration, characteristic feature of the OIR model. Additionally, honokiol enhanced physiological revascularization of the retinal vascular plexuses. Since honokiol suppresses multiple pathways activated by HIF, in addition to the VEGF signaling, it may provide advantages over current treatments utilizing specific VEGF antagonists for ocular neovascular diseases and cancers.

1. Introduction

Retinal neovascular diseases such as diabetic retinopathy, retinal vein occlusions, and retinopathy of prematurity develop due to diverse predicaments damaging retinal blood vessels. In the case of diabetic retinopathy, the underlying cause is hyperglycemia; in retinal vein occlusions, obstruction of vascular flow increases hydrostatic pressure and subsequently reduces perfusion; and in retinopathy of prematurity, exposure to high levels of oxygen at a particular stage of retinal vascular development. These primary insults damage retinal vessels, generating poorly perfused areas with retinal ischemia. Therefore, these diseases are collectively also referred to as ischemic retinopathies. Ocular ischemia is also observed during neovascular age-related macular degeneration and glaucoma. Irrespective of the different underlying reasons for ischemic retinopathies, they all ultimately lead to retinal hypoxia [1]. Hypoxia allows translocation of HIF-α subunit to the nucleus, its dimerization with the HIF-1β/ARNT subunit, and recruitment of other transcriptional co-activators. An active HIF-α/β heterodimeric transcription factor then binds to the hypoxia-response-element (HRE) present in the promoters of hypoxia response genes causing overexpression of vascular endothelial growth factor (VEGF) and other pro-angiogenic factors. The pathological neovascularization initiated by these pro-angiogenic factors lack tight junctions and hence leak plasma into surrounding tissues causing retinal detachment and severe vision loss.

A number of antiangiogenic therapies targeting VEGF (e.g. Ranibizumab, Pegaptanib, Aflibercept, Bevacizumab, etc.) have been approved for the treatment of neovascular diseases of eye and cancer [2]. Although specific VEGF antagonists have revolutionized the treatment of these diseases [3–6], a major improvement in the vision is observed in approximately half of the patients with age-related macular degeneration [5,6]. Further, all anti-VEGF treatments

Abbreviations: HIF, hypoxia inducible factor; HRE, hypoxia response element; PHD, prolyl hydroxylation domain; VHL, von Hippel–Lindau; VEGF, vascular endothelial growth factor; OIR, oxygen-induced retinopathy; P, postnatal day; IP, intraperitoneal.

* Corresponding author. Address: Division of Pharmaceutical Sciences, School of Pharmacy, University of Missouri-Kansas City, 2464 Charlotte Street, Kansas City, MO 64108-2718, USA. Fax: +1 816 235 5779.
E-mail address: mukherjim@umkc.edu (M. Mukherji).

[1] These authors contributed equally to this work.

0006-291X/$ - see front matter © 2013 Elsevier Inc. All rights reserved.
http://dx.doi.org/10.1016/j.bbrc.2013.07.118

require repeated injections of VEGF antagonists at a high cost, and yet, only offer temporary respite from vascular leakage resulting in partial clinical success. This lack of efficacy of anti-VEGF therapy in this process is possibly due to implication of the HIF pathway-mediated expression of other pro-angiogenic factors like platelet-derived growth factor-B, stromal cell-derived factor 1, erythropoietin, etc. [7]. The relative inefficiency of anti-VEGF therapy may also be due to temporal nature of the angiogenic process. Thus, possible future approaches to successfully control pathological neovascularization may rely on blocking some master modulator, such as the HIF pathway.

Thus characterization of novel HIF inhibitors can have considerable therapeutic impact on pathological neovascularization in ischemic diseases and cancers [8,9]. Recent screening of compounds that are in clinical practice identified cardiac glycosides (e.g. digoxin, proscillaridin A, and ouabain) and anthracyclines (e.g. doxorubicin and daunorubicin) as potent HIF inhibitors [10,11]. Since activation of the HIF pathway is the underlying cause of ocular neovascularization, both digoxin and doxorubicin are examined for the treatment of ischemic ocular retinopathies [12,13]. We have recently shown that honokiol, a biphenolic phytochemical extracted from the *Magnolia* genus, is also a potent inhibitor of the HIF pathway [14]. Here we evaluate the toxicity and efficacy of digoxin, doxorubicin, and honokiol as HIF inhibitors in retinal pigment epithelial cell lines. Further, we show for the first time that administration of honokiol reduces retinal neovascularization in the OIR mouse model. Honokiol also prevents the oxygen-induced central retinal vaso-obliteration, the characteristic feature of the OIR model.

2. Materials and methods

2.1. Cell culture and exposure of cells to hypoxia

Human retinal pigment epithelial cell lines (D407 and ARPE19) were used to evaluate the efficacy of digoxin, doxorubicin, and honokiol. The D407 and ARPE19 cells were cultured as previously reported [14,15]. All the drugs used in this study were prepared in DMSO. The inhibition studies were performed by adding 1 μM of digoxin or 1 μM of doxorubicin or 20 μM of honokiol to the cells. In the control samples 0.1% of DMSO, corresponding to the DMSO concentration in the cells treated with highest inhibitor concentration, was added. Cells were exposed to hypoxic condition in a bactron anaerobic chamber as previously reported [14,15]. Cell lysis for RNA extraction was performed after exposure to hypoxia for 12 h in the hypoxic chamber to avoid any exposure of cells to normoxic conditions.

2.2. RNA extraction from cells and quantitative real-time PCR analysis

RNA was extracted from cells and the quantitative real-time PCR (qPCR) reactions were performed as described in our earlier publications [14,15]. The qPCR reactions were performed in biological and experimental duplicates. Ribosomal protein L32 was utilized as an internal control to normalize the sample to obtain ΔC_t value. $2^{-\Delta\Delta Ct}$ method was used to analyze the relative gene expression levels.

2.3. Cell viability assay

Cell viability assay was performed to determine the IC_{50} value of each HIF inhibitor. Briefly, for these experiments, 10,000 cells/well were plated into 96-well plates and exposed to varying concentrations (six replicates at each concentration) of HIF inhibitors for 24 h. Following this, the number of viable cells was calculated using the Premixed WST-1 Cell Proliferation Reagent according to the manufacturer's protocol (Clontech, Mountain View, CA). This kit provides a method to measure cell proliferation based on the enzymatic cleavage of the tetrazolium salt (WST-1) to a water-soluble formazan dye, which was detected by absorbance at 450 nm using a micro titer plate reader (Analyst GT, Molecular Devices, Sunnyvale, CA). The amount of formazan formed is directly proportional to the number of viable cells. The IC_{50} values of the three compounds were calculated using the GraphPad Prism software.

2.4. Mouse model of oxygen-induced retinopathy

C57BL/6J mice, purchased from Jackson Laboratories (Bar Harbor, ME), were used for these experiments. All experimental procedures were approved by the University of Kansas Medical Center Institutional Animal Care and Use Committee. All mice were kept in a 12 h light–dark cycle at ambient room temperature (i.e. 19–22 °C). Mice were maintained on a standard diet for breeding (8626 rodent diet; Harlan Laboratories, Indianapolis, IN), with chow and water available ad libitum. For the OIR model, the newborn pups at post-natal day 7 (P7) along with their mother were transferred to a chamber supplied with 75 ± 2% oxygen as described [16], under continual monitoring with a ProOx 110 oxygen controller (Biospherix, Ltd., Lacona, NY) for 120 h. On P12, the mice were returned to the room air, and were given daily intraperitoneal (IP) injection of vehicle (12.5% polyethylene glycol 400 in 1 × PBS) or 10–20 mg/kg of honokiol dissolved in the vehicle.

2.5. Whole mount fluorescent staining

Mice were anesthetized on P17 by IP injection of ketamine (1%), xylazine (0.1%), and sodium chloride (0.9%) in a concentration of 0.1 mL/10 g mouse body weight. After induction of deep anesthesia, eyes were carefully harvested and fixed in 4% paraformaldehyde for 24 h at 4 °C. A microscope was used to dissect the cornea with a circumferential limbal incision, followed by removal of the lens, vitreous, and neural retina. Retinal cups were permeabilized overnight in 0.5% Triton X-100 and 1% BSA in 1 × PBS. After washing, retinae were incubated in 10 μg/mL isolectin GS-IB4, Alexa Flour 563 conjugate (Life Technologies, Grand Island, NY) in 1 mM $CaCl_2$, 2 mM NaN_3, 1 × PBS overnight at room temperature according to established protocols [17]. After final washes with 1 × PBS, retinae were flat mounted in an anti-fade medium (Southern Biotech, Birmingham, AL).

2.6. Quantification of retinal neovascularization

Fluorescent images of the stained retinae were taken at 4 × magnification using a Nikon Eclipse 80i fluorescent microscope and Nikon Elements software (Nikon, Tokyo, Japan). Adobe Photoshop CS6 software was used to photo-merge images (3–5 images/retina) prior to analysis. Retinal neovascularization and vaso-obliteration were quantified as reported earlier [17,18]. Both neovascularization and vaso-obliteration are represented as % of total retinal area. Vaso-obliteration was manually measured using ImageJ software (http://rsbweb.nih.gov/ij/). The total retinal area and vaso-obliteration quantifications were obtained using Adobe Photoshop CS6. Neovascularization was quantified using a semi-automated computer program SWIFT_NV [18], which is a set of macros run on NIH's image J software. SWIFT_NV has a pixel cut-off value specific for each retina, based on the total retinal area, which excludes small vessel branch points from neovascularization quantification. SWIFT_NV divides the retinal image into four quadrants. During the neovascularization quantification of each quadrant, artifacts like hyper fluorescent retinal ends, hyaloid vasculature, and cellular debris were excluded from the analysis. Further, a threshold

was set to highlight the neovascular tufts while excluding normal vasculature from the quantification. SWIFT_NV finally generated a stitched image highlighting the neovascular tufts on the original retinal image and gave the neovascularization area. The data is represented as means ± S.E. Students' *t*-test was performed to evaluate the strength of significance. *P*-values less than 0.05 were considered as significant.

3. Results and discussions

3.1. Evaluation of IC_{50} values of HIF inhibitors

HIF pathway plays a critical role in the pathobiology of a number of oxygen-dependent retinal diseases such as ocular hemangioblastoma, diabetic retinopathy, retinal vein occlusions, glaucoma, age-related macular degeneration, and retinopathy of prematurity [1]. We have shown in our earlier studies that honokiol, a phytochemical isolated from the *Magnolia* species, is a potent HIF inhibitor [19]. Recent studies have demonstrated that a number of therapeutic agents like digoxin and doxorubicin are also HIF inhibitors [11,20–22]. Therefore, initially we compared the toxicity and efficacy of digoxin, doxorubicin, and honokiol as HIF inhibitors.

Since retinal pigment epithelial cells are one of the major cell constituents and secretors of VEGF in the retina [23], two human retinal pigment epithelial cell lines (D407 and ARPE19) were selected to determine the IC_{50} values of compounds [24,25]. For these viability studies, cells were exposed to varying concentrations of the drugs (0.48 nM to 30 μM for digoxin and doxorubicin; 10–800 μM for honokiol) for 24 h. The number of viable cells was calculated using the Premixed WST-1 Cell Proliferation Reagent as described in the materials and methods. Digoxin showed IC_{50} value of 285.40 nM (Fig. 1A), doxorubicin showed IC_{50} value of 402.90 nM (Fig. 1B), while in the case of honokiol the IC_{50} value was 187.40 μM for ARPE19 cells (Fig. 1C). Similar results were also obtained for D407 cell line (data not shown). These results suggest that honokiol is far less toxic compound compared to digoxin and doxorubicin for human retinal pigment epithelial cells, and can be used at higher concentrations than digoxin and doxorubicin. Our results corroborate well with the use of honokiol as a neuroprotective agent [26].

3.2. Transcription inhibition of direct HIF targets by digoxin, doxorubicin, and honokiol

To evaluate the efficacy of digoxin, doxorubicin, and honokiol as HIF inhibitors, we evaluated the transcription of a number of direct HIF-dependent genes under hypoxic conditions in the presence and absence of drugs. Based on the IC_{50} values and the data from earlier studies [11,20], 1 μM of digoxin and doxorubicin and 20 μM of honokiol were used to perform the comparative inhibition studies. ARPE19 cells were treated with the HIF inhibitors for 12 h at ~70% confluency under hypoxia. The RNA extraction, cDNA synthesis, and qPCR analysis were performed as described in the materials and methods section. Since we have shown the induction of a number of direct HIF targets (e.g. *JMJD1A*, *JMJD2B*, *JMJD2C*, *JARID1B*, *VEGF*, and *GLUT1*) under hypoxic conditions using human retinal pigment epithelial cell lines [14,15], we focused on the transcription levels of these genes for comparative studies. Consistent with our previous studies, following exposure to hypoxia, we observed strong induction of all the selected direct HIF targets (e.g. *JMJD1A* (2.4-fold), *JMJD2B* (3.1-fold), *JMJD2C* (1.5-fold), *JARID1B* (1.6-fold), *VEGF* (3.8-fold), and *GLUT1* (3.7-fold)) under hypoxia relative to normoxic conditions in ARPE19 cells (Fig. S1).

However, cells treated with 1 μM of digoxin and doxorubicin, which is ~3 times their IC_{50} values, showed significant inhibition

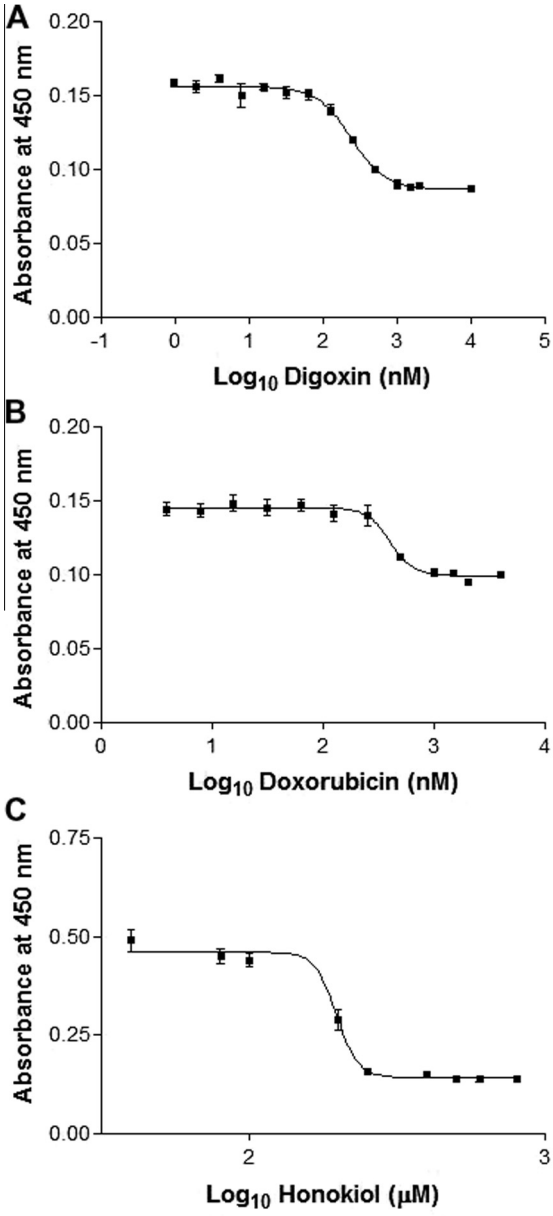

Fig. 1. Determination of IC_{50} values for HIF inhibitors. ARPE19 cells were treated with varying concentrations of drugs (0.48 nM-30 μM of digoxin or doxorubicin, 10–800 μM of honokiol) for 24 h. The number of viable cells was calorimetrically calculated using the Premixed WST-1 Cell Proliferation Reagent by detecting the amount of formazan formed at 450 nm. Plotting the absorbance at 450 nm vs. $\log_{10}$ value of drug concentrations yielded the IC_{50} of 285.40 nM, 402.90 nM, and 187.40 μM for digoxin (A), doxorubicin (B), and honokiol (C), respectively.

of hypoxic induction of all the selected HIF targets (e.g. for digoxin *JMJD1A* (0.4-fold), *JMJD2B* (1.0-fold), *JMJD2C* (1.0-fold), *JARID1B* (1.1-fold), *VEGF* (0.7-fold), and *GLUT1* (0.4-fold); while for doxorubicin *JMJD1A* (0.3-fold), *JMJD2B* (0.6-fold), *JMJD2C* (0.3-fold), *JARID1B* (0.7-fold), *VEGF* (0.3-fold), and *GLUT1* (0.3-fold)) under drug treated hypoxic conditions relative to untreated hypoxic conditions in ARPE19 cells (Fig. S1). At the same time, treatment of cells with 20 μM honokiol, which is ~1/9th of the IC_{50} value for ARPE19 cells, showed significant inhibition of transcription of selected HIF targets (e.g. *JMJD1A* (0.2-fold), *JMJD2B* (0.6-fold), *JMJD2C* (0.4-fold), *JARID1B* (0.5-fold), *VEGF* (0.2-fold), and *GLUT1* (0.2-fold)) in ARPE19 cells (Fig. S1). Although treatment with all three compounds resulted in lowering the transcription levels of selected HIF targets, bringing them back to or below their normoxic levels, it is

interesting to note that honokiol showed better efficacy as HIF inhibitor (note that honokiol was used at ~1/9th of the IC_{50} value for ARPE19 cells, while digoxin and doxorubicin were used at ~3 times higher concentrations than their IC_{50} values). Similar results with respect to transcription inhibition of HIF targets were observed at as low as 5 μM concentration of honokiol [14]. These results suggest that honokiol has a better safety to efficacy profile as a HIF inhibitor, compared to digoxin and doxorubicin, and can be used for the treatment of various ischemic ocular diseases.

3.3. Honokiol inhibits pathological retinal neovascular tuft formation in oxygen-induced retinopathy mouse model

Considering both digoxin and doxorubicin have been examined for the treatment of ischemic ocular retinopathies [12,13], we evaluated the efficacy of honokiol as a treatment option for these diseases in the OIR mouse model (Fig. 2). This model has been extensively used to study the regulation of angiogenic factors, vascular pathogenesis, and the efficacy of antiangiogenic compounds [12,27]. In this model, the P7 mouse pups are placed in 75% oxygen for 5 days. Exposure of 7 day old pups to high levels of oxygen inhibits retinal vessel growth and causes significant oxygen-induced central retinal vessel loss (i.e. vaso-obliteration). At P12, the mice are returned to room air and the non-perfused central retina becomes relatively hypoxic. This activates the HIF pathway and pathological neovascularization, which is maximal at P17 [17].

For our experiments, mouse pups were divided into three separate groups; group 1: vehicle-treated hyperoxia-exposed mice (sham-treated positive control), group 2: 10 mg/kg honokiol-treated hyperoxia-exposed mice (drug-treated), and group 3: 20 mg/kg honokiol-treated hyperoxia-exposed mice (drug-treated). Mice from all groups that had undergone the OIR procedure, were returned to room air on P12 and vehicle or 10–20 mg/kg of honokiol dissolved in vehicle was injected daily (from P12 to P16) by IP route (Fig. 2). The extent of neovascularization at P17 was measured on retinal flat mounts using a computer-aided program as described in the materials and methods and Fig. S2.

In total, 55 retinae from 35 P17 mice were analyzed for pathological retinal neovascular tuft formation. Note that some retinae were damaged during the processing, and therefore, were not included in the analysis. Further, the mice that weighed less than 6 g on P17 were also excluded from the analysis according to a previous publication [17]. The retinae from vehicle-treated mice (group 1) demonstrated that 4.38 ± 0.95% of the total retinal area was covered by neovascular tufts (Table 1 and, Fig. 3B). The neovascular tufts were evident by the thickening of the blood vessels and heightened staining of the vasculature with the fluorescent dye. However, fluorescent imaging studies of retinae from P17 mice from groups 2 and 3 demonstrated that daily IP injection of 10–20 mg/kg of honokiol starting on P12 significantly (~35%) reduced neovascular tufts, the clinical manifestations of the retinal neovascular response (Fig. 3C–D). Interestingly, we did not observe a difference (2.73 ± 0.65% with 10 mg/kg of honokiol vs. 2.71 ± 0.62% with 20 mg/kg of honokiol) in the neovascular tufts formation in mice treated with 10 or 20 mg/kg of honokiol, suggesting that saturation of therapeutic concentration of honokiol in the retina was reached at 10 mg/kg OIR mice. Initial experiments with 0.2 and 2 mg/kg of honokiol did not have a significant effect on neovascularization in OIR mice (data not shown). Students' *t*-test was performed between the vehicle-treated and honokiol-treated groups which gave a *p*-value of <0.01, suggesting that our results are statistically highly significant. Further, since no report with toxicity studies of honokiol in very young mouse pups was found in the literature, we monitored the weight of pups daily from P12 to P17. To this end, no weight difference was noted between the vehicle-treated or honokiol-treated groups (data not shown), and the P17 mice appeared normal with similar sizes (Fig. S3).

3.4. Honokiol promotes physiological revascularization in oxygen-induced retinopathy mouse model

To assess the vascular repair and physiological revascularization mechanisms after hyperoxia-induced vaso-obliteration, the avascular areas were quantified. Avascular areas appear as dark regions that were not perfused by fluorescent dye. The vehicle-treated ischemic retinae from group 1 mice exhibited large avascular areas (Fig. 3C). However, the vaso-obliterated areas in honokiol-treated retinae from groups 2 and 3 were reduced by ~10–25%, compared with the vehicle-treated ischemic retinae from group 1 on P17 (Fig. 3F and I). Students' *t*-test comparing vehicle-treated mice to honokiol-treated mice found $p < 0.02$ confirming the significance of our results. Moreover, since the vascular morphology of honokiol treated retinae appears more normal than the vehicle-treated ischemic retinae (Fig. 3), we conclude that daily IP injections of honokiol promoted vascular repair and physiological revascularization. Taken together, these results demonstrate that honokiol is an effective therapeutic agent for the treatment of ischemic ocular neovascularization.

Neovascularization in the eye is one of the major causes of blindness in people of all ages (WHO, 2011). Worldwide, 2.5 million people experience vision loss due to diabetic retinopathy, whereas the age-related macular degeneration affects 25–30 million people. Other neovascular ocular diseases such as retinopathy of prematurity and retinal vascular occlusions are less prevalent but extremely debilitating with retinopathy of prematurity representing the major cause of blindness in children. Extensive studies have identified promising anti-VEGF agents to treat these debilitating diseases. However, a major improvement in the vision is

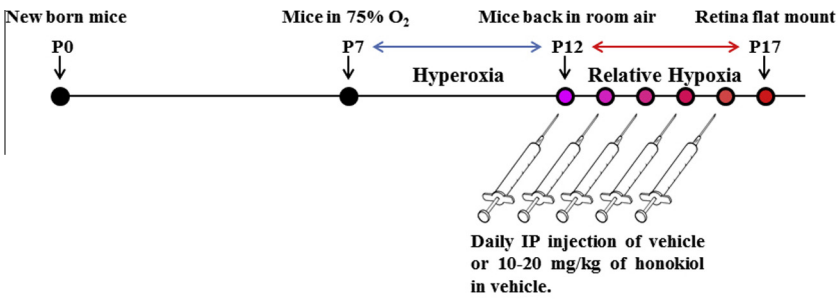

Fig. 2. Schematic representation of experimental conditions used to evaluate the efficacy of honokiol in the OIR mouse model. Mice were placed in 75% oxygen between P7 and 12, and then returned to room air between P12 and 17. This results in central vaso-obliteration and retinal ischemia, initiating the pathologic growth of blood vessels and neovascular tufts. Daily IP injections of vehicle or 10–20 mg/kg of honokiol dissolved in vehicle were administered from P12 to 16. On P17, mice were sacrificed and eyes were enucleated. Following fixation and fluorescent staining, retinae were flat mounted for imaging studies.

Table 1
Table showing neovascular tufts and avascular areas in the mice retinae from groups 1–3.

	Neovascular tufts (of total retinal area) ± S.E.	Avascular area (of total retinal area) ± S.E.
Group 1: sham-treated positive control, vehicle-treated hyperoxia-exposed mice	4.38 ± 0.95%	22.16 ± 1.25%
Group 2: low dose drug-treated, i.e. 10 mg/kg honokiol-treated hyperoxia-exposed mice	2.73 ± 0.65%	19.53 ± 1.33%
Group 3: high dose drug-treated, *i.e.* 20 mg/kg honokiol-treated hyperoxia-exposed mice	2.71 ± 0.62%	16.72 ± 1.21%

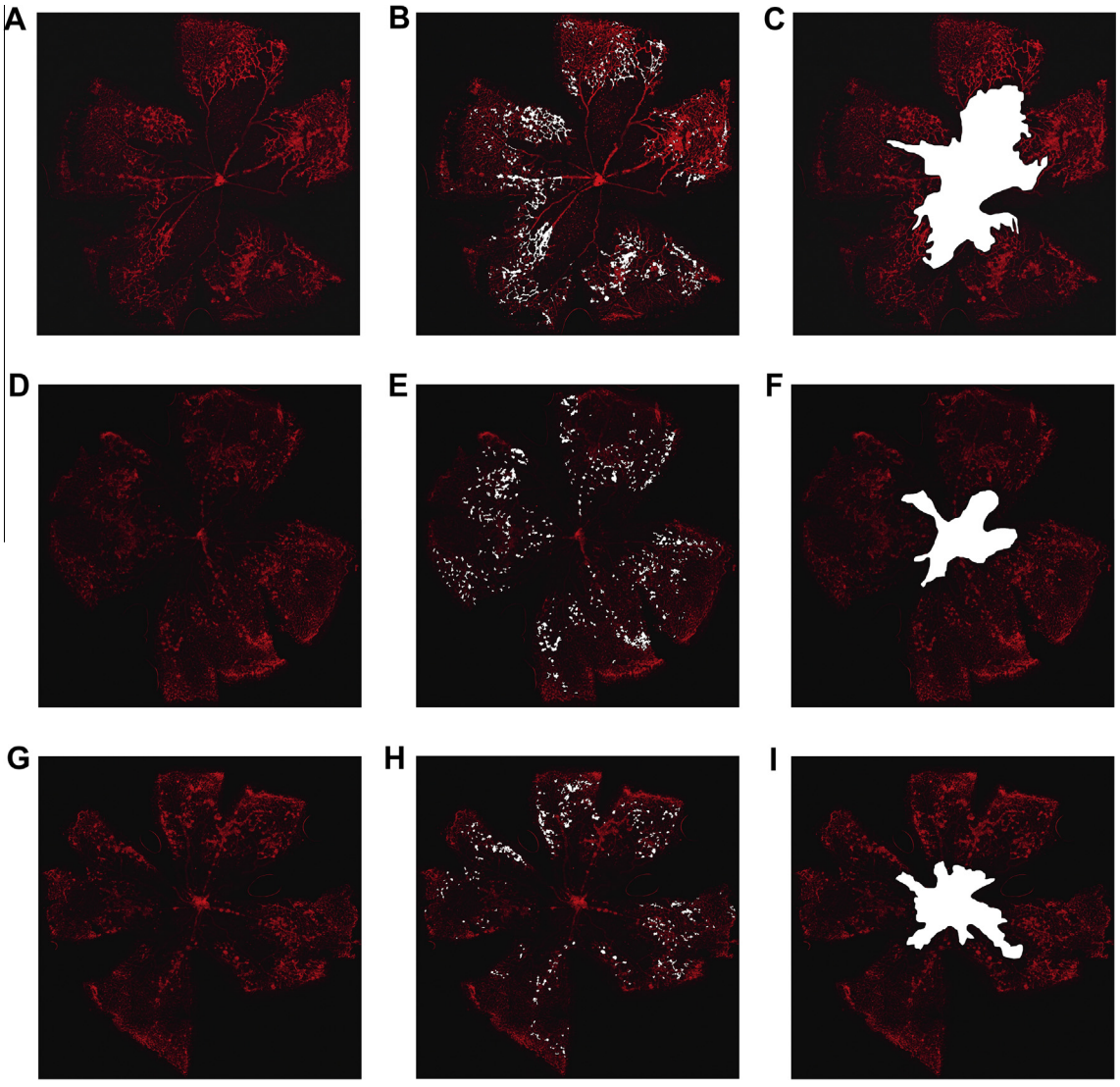

Fig. 3. Fluorescent imaging of the retinal flat mounts showing blood vasculature (left column), neovascular tufts (middle column), and avascular areas (right column), from group 1, i.e. sham-treated hyperoxia-exposed mice (A–C), group 2, i.e. 10 mg/kg honokiol-treated hyperoxia-exposed mice (D–F), and group 3, i.e. 20 mg/kg honokiol-treated hyperoxia-exposed mice (G–I).

observed in approximately half of the patients with age-related macular degeneration receiving Ranibizumab [5,6]. Further, anti-VEGF therapies only offer temporary respite from vascular leakage at a very high cost. It is because of these factors that there remains an unmet medical need to develop a more cost-effective small molecule drug with new mechanism of action which could inhibit pathological neovascularization in patients with ocular diseases and cancers.

In the present study, we show that honokiol inhibits the HIF pathway-mediated expression of pro-angiogenic genes, including VEGF. Honokiol has a better safety to efficacy profile as HIF inhibitor than digoxin and doxorubicin. We also show for the first time that daily IP injection of honokiol at P12 in an OIR mouse model significantly inhibits pathological retinal neovascular tuft formation at P17. Administration of honokiol prevents the oxygen-induced central retinal vaso-obliteration, and promotes vascular recovery in the ischemic retina. Finally, our results demonstrate that honokiol, which in its crude form has been used for thousands of years in the traditional Japanese and Chinese medicine for other conditions, can also be used to inhibit pathological neovascularization in patients with ocular diseases.

Acknowledgments

This research was funded by UMKC internal support in the form of bridge fund to MM and GAF fellowship to DTV. We thank Dr L. E. Smith, Harvard Medical School, for the generous gift of SWIFT_NV. The authors would also like to thank Dr. Kun Cheng for allowing us to use the real-time qPCR instrument.

Appendix A. Supplementary data

Supplementary data associated with this article can be found, in the online version, at http://dx.doi.org/10.1016/j.bbrc.2013.07.118.

References

[1] P.A. Campochiaro, Ocular neovascularization, J. Mol. Med. (Berl.) 91 (2013) 311–321.
[2] M.W. Stewart, The expanding role of vascular endothelial growth factor inhibitors in ophthalmology, Mayo Clin. Proc. 87 (2012) 77–88.
[3] L.P. Aiello, E.A. Pierce, E.D. Foley, H. Takagi, H. Chen, L. Riddle, N. Ferrara, G.L. King, L.E. Smith, Suppression of retinal neovascularization in vivo by inhibition of vascular endothelial growth factor (VEGF) using soluble VEGF-receptor chimeric proteins, Proc. Natl. Acad. Sci. USA 92 (1995) 10457–10461.
[4] H. Ozaki, M.S. Seo, K. Ozaki, H. Yamada, E. Yamada, N. Okamoto, F. Hofmann, J.M. Wood, P.A. Campochiaro, Blockade of vascular endothelial cell growth factor receptor signaling is sufficient to completely prevent retinal neovascularization, Am. J. Pathol. 156 (2000) 697–707.
[5] D.M. Brown, P.K. Kaiser, M. Michels, G. Soubrane, J.S. Heier, R.Y. Kim, J.P. Sy, S. Schneider, Ranibizumab versus verteporfin for neovascular age-related macular degeneration, N. Engl. J. Med. 355 (2006) 1432–1444.
[6] P.J. Rosenfeld, D.M. Brown, J.S. Heier, D.S. Boyer, P.K. Kaiser, C.Y. Chung, R.Y. Kim, Ranibizumab for neovascular age-related macular degeneration, N. Engl. J. Med. 355 (2006) 1419–1431.
[7] S.X. Zhang, J.X. Ma, Ocular neovascularization: Implication of endogenous angiogenic inhibitors and potential therapy, Prog. Retin Eye Res. 26 (2007) 1–37.
[8] G.L. Semenza, HIF-1 inhibitors for cancer therapy: from gene expression to drug discovery, Curr. Pharm. Des. 15 (2009) 3839–3843.
[9] H.S. Ban, Y. Uto, H. Nakamura, Hypoxia-inducible factor inhibitors: a survey of recent patented compounds (2004–2010), Expert Opin. Ther. Patient 21 (2011) 131–146.
[10] H. Zhang, D.Z. Qian, Y.S. Tan, K. Lee, P. Gao, Y.R. Ren, S. Rey, H. Hammers, D. Chang, R. Pili, C.V. Dang, J.O. Liu, G.L. Semenza, Digoxin and other cardiac glycosides inhibit HIF-1alpha synthesis and block tumor growth, Proc. Natl. Acad. Sci. USA 105 (2008) 19579–19586.
[11] K. Lee, D.Z. Qian, S. Rey, H. Wei, J.O. Liu, G.L. Semenza, Anthracycline chemotherapy inhibits HIF-1 transcriptional activity and tumor-induced mobilization of circulating angiogenic cells, Proc. Natl. Acad. Sci. USA 106 (2009) 2353–2358.
[12] T. Yoshida, H. Zhang, T. Iwase, J. Shen, G.L. Semenza, P.A. Campochiaro, Digoxin inhibits retinal ischemia-induced HIF-1alpha expression and ocular neovascularization, FASEB J. 24 (2010) 1759–1767.
[13] T. Iwase, J. Fu, T. Yoshida, D. Muramatsu, B. Oveson, B. Han, M. Wu, G.L. Semenza, J. Hanes, P.A. Campochiaro, Safe and effective polymeric-doxorubicin conjugate nanoparticles for prolonged antiangiogenic activity in the Eye, ARVO Annual Meeting E-Abstract 3008 (2012).
[14] D.T. Vavilala, V.K. Chaithanya Ponnaluri, R.K. Vadlapatla, D. Pal, A.K. Mitra, M. Mukherji, Honokiol inhibits HIF pathway and hypoxia-induced expression of histone lysine demethylases, Biochem. Biophys. Res. Commun. 422 (2012) 369–374.
[15] V.K. Ponnaluri, R.K. Vadlapatla, D.T. Vavilala, D. Pal, A.K. Mitra, M. Mukherji, Hypoxia induced expression of histone lysine demethylases: implications in oxygen-dependent retinal neovascular diseases, Biochem. Biophys. Res. Commun. 415 (2011) 373–377.
[16] L.E. Smith, E. Wesolowski, A. McLellan, S.K. Kostyk, R. D'Amato, R. Sullivan, P.A. D'Amore, Oxygen-induced retinopathy in the mouse, Invest. Ophthalmol. Vis. Sci. 35 (1994) 101–111.
[17] K.M. Connor, N.M. Krah, R.J. Dennison, C.M. Aderman, J. Chen, K.I. Guerin, P. Sapieha, A. Stahl, K.L. Willett, L.E. Smith, Quantification of oxygen-induced retinopathy in the mouse: a model of vessel loss, vessel regrowth and pathological angiogenesis, Nat. Protoc. 4 (2009) 1565–1573.
[18] A. Stahl, K.M. Connor, P. Sapieha, K.L. Willett, N.M. Krah, R.J. Dennison, J. Chen, K.I. Guerin, L.E. Smith, Computer-aided quantification of retinal neovascularization, Angiogenesis 12 (2009) 297–301.
[19] D.T. Vavilala, V.K. Ponnaluri, R.K. Vadlapatla, D. Pal, A.K. Mitra, M. Mukherji, Honokiol inhibits HIF pathway and hypoxia-induced expression of histone lysine demethylases, Biochem. Biophys. Res. Commun. 422 (2012) 369–374.
[20] C.C. Wong, H. Zhang, D.M. Gilkes, J. Chen, H. Wei, P. Chaturvedi, M.E. Hubbi, G.L. Semenza, Inhibitors of hypoxia-inducible factor 1 block breast cancer metastatic niche formation and lung metastasis, J. Mol. Med. (Berl.) 90 (2012) 803–815.
[21] G.L. Semenza, Evaluation of HIF-1 inhibitors as anticancer agents, Drug Discov. Today 12 (2007) 853–859.
[22] G. Melillo, Targeting hypoxia cell signaling for cancer therapy, Cancer Metastasis Rev. 26 (2007) 341–352.
[23] M.G. Slomiany, S.A. Rosenzweig, IGF-1-induced VEGF and IGFBP-3 secretion correlates with increased HIF-1 alpha expression and activity in retinal pigment epithelial cell line D407, Invest. Ophthalmol. Vis. Sci. 45 (2004) 2838–2847.
[24] P. Geisen, J.R. McColm, B.M. King, M.E. Hartnett, Characterization of barrier properties and inducible VEGF expression of several types of retinal pigment epithelium in medium-term culture, Curr. Eye Res. 31 (2006) 739–748.
[25] F. Forooghian, R. Razavi, L. Timms, Hypoxia-inducible factor expression in human RPE cells, Br. J. Ophthalmol. 91 (2007) 1406–1410.
[26] V. Praveen Kumar, R. Gajendra Reddy, D.D. Vo, S. Chakravarty, S. Chandrasekhar, R. Gree, Synthesis and neurite growth evaluation of new analogues of honokiol, a neolignan with potent neurotrophic activity, Bioorg. Med. Chem. Lett. 22 (2012) 1439–1444.
[27] M. DeNiro, A. Al-Halafi, F.H. Al-Mohanna, O. Alsmadi, F.A. Al-Mohanna, Pleiotropic effects of YC-1 selectively inhibit pathological retinal neovascularization and promote physiological revascularization in a mouse model of oxygen-induced retinopathy, Mol. Pharmacol. 77 (2010) 348–367.